

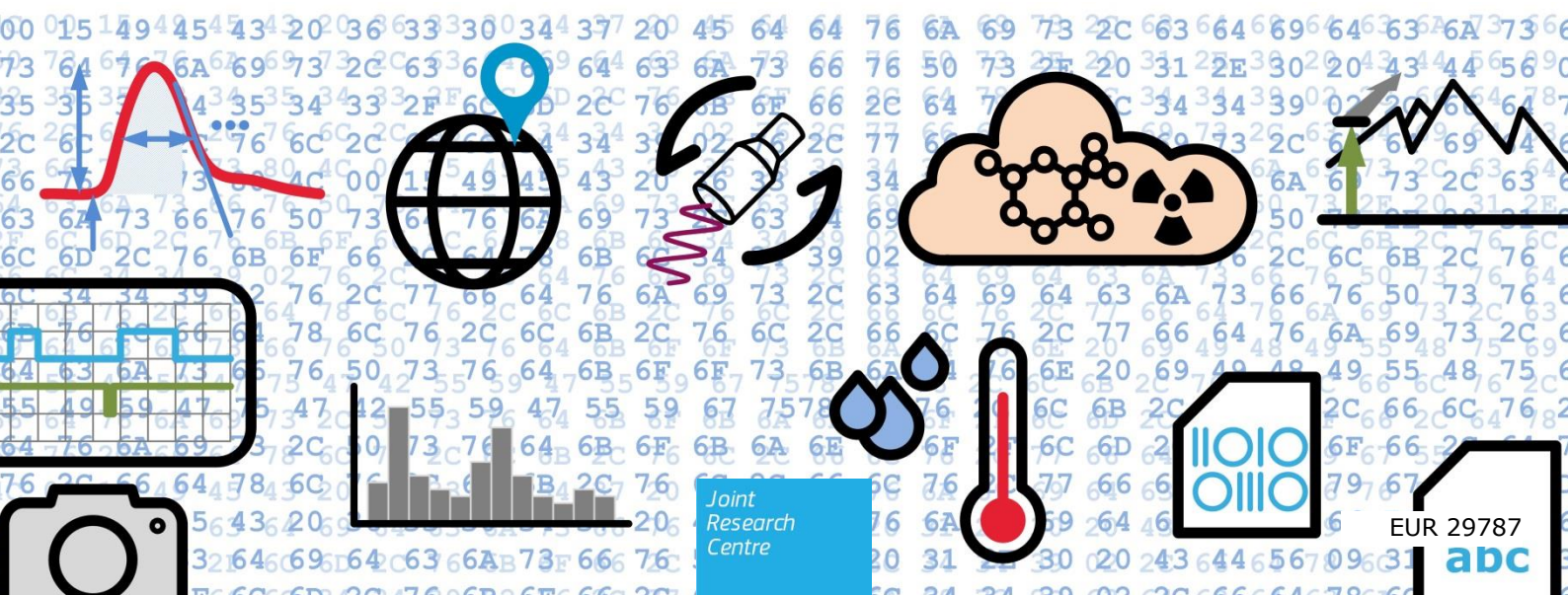
## JRC TECHNICAL REPORTS

# Performance of the IEC 63047 demonstration device

*ERNCIP Thematic Group  
Radiological and Nuclear  
Threats to Critical  
Infrastructure*

Paepen, J.  
Lutter, G.  
Schneider, F. E.  
Garcia Rosas, F.  
Röning, J.

2019



This publication is a Scientific Information Systems and Databases report by the Joint Research Centre (JRC), the European Commission's science and knowledge service. It aims to provide evidence-based scientific support to the European policymaking process. The scientific output expressed does not imply a policy position of the European Commission. Neither the European Commission nor any person acting on behalf of the Commission is responsible for the use that might be made of this publication.

**Contact information**

Name: Jan Paepen  
Address: JRC-Geel, Retieseweg 111, B-2440 Geel, Belgium  
Email: [jan.paepen@ec.europa.eu](mailto:jan.paepen@ec.europa.eu)  
Tel.: +32 14 571329

**EU Science Hub**

<https://ec.europa.eu/jrc>

JRC116872

EUR 29787

PDF      ISBN 978-92-76-08684-0      ISSN 1831-9424      doi:10.2760/041774

Luxembourg: Publications Office of the European Union, 2019

© European Atomic Energy Community, 2019

The reuse policy of the European Commission is implemented by Commission Decision 2011/833/EU of 12 December 2011 on the reuse of Commission documents (OJ L 330, 14.12.2011, p. 39). Reuse is authorised, provided the source of the document is acknowledged and its original meaning or message is not distorted. The European Commission shall not be liable for any consequence stemming from the reuse. For any use or reproduction of photos or other material that is not owned by the EU, permission must be sought directly from the copyright holders.

All content © European Atomic Energy Community, 2019, except:

*page 7, Figure 3, 2019. Source: Google*

*page 15, Figure 13 and page 18, Figure 14, 2019. Source: Fraunhofer FKIE*

How to cite this report: Paepen, J., Lutter, G., Schneider, F. E., Garcia Rosas, F., Röning, J., *Performance of the IEC 63047 demonstration device*, EUR 29787, Publications Office of the European Union, Luxembourg, 2019, ISBN 978-92-76-08684-0, doi:10.2760/041774, JRC116872.

# Contents

Abstract .....	3
1 Introduction.....	4
2 IEC 63047 demonstration device .....	5
2.1 Components.....	5
2.2 Operation .....	6
2.3 Test results.....	7
2.3.1 Positioning accuracy.....	7
2.3.2 Performance of the radiation detector in laboratory conditions.....	8
2.3.3 Field tests.....	14
3 Integration in ROS.....	15
3.1 ROS framework .....	15
3.2 ROS device driver node .....	16
3.3 ROS OCU driver node .....	17
3.4 Performance test .....	17
Conclusions .....	19
References .....	20
List of abbreviations and definitions .....	21
List of figures.....	22
List of tables .....	23
Annexes .....	24
Annex 1. IEC 63047 data acquired during field tests .....	24

**Authors**

Paepen, J., European Commission, Joint Research Centre (JRC), Geel, Belgium

Lutter, G., European Commission, Joint Research Centre (JRC), Geel, Belgium

Garcia Rosas, F., Fraunhofer FKIE, Wachtberg, Germany

Schneider, F. E., Fraunhofer FKIE, Wachtberg, Germany

Röning, J., University of Oulu, Oulu, Finland

**NOTE**

The 'demonstration device' and its components (hardware and software) described in this document are to be considered as examples only. Similar systems may be built from alternative products.

## **Abstract**

The International Electrotechnical Commission (IEC) published a new international standard, IEC 63047, specifying a data format for list-mode digital data acquisition used in radiation detection and measurement. IEC 63047 was developed under the lead of the JRC in the frame of Commission mandate M/487 issued by The Commission's Directorate-General for Internal Market, Industry, Entrepreneurship and SMEs (DG GROW). The pre-normative research for this standard was performed by the European Reference Network for Critical Infrastructure Protection (ERNCIP), in particular its Thematic Group on Radiological and Nuclear threats to critical infrastructure.

The JRC and the ERNCIP RN TG promote the use of the standard in a wide range of applications involving radiation detection and measurement: novel detector technologies, nuclear security, reachback/expert support and robotics. The standard can be applied to CBRNE detection equipment because it includes features to represent data from any kind of sensor, including geolocation.

The JRC developed a demonstration device from off-the-shelf components and proposed and tested an open-source solution for encoding and decoding binary IEC 63047 messages. The ERNCIP RN Robotics subgroup developed a software interface between IEC 63047 and the Robot Operating System (ROS). The demonstration device consists of a single-board computer, a spectrometric radiation detector and a Global Navigation Satellite System (GNSS) receiver which enables real-time-kinematics to achieve centimetre accurate positioning.

Tests performed at the JRC-Geel site assessed the performance of the demonstration device in laboratory and field conditions. Using real-time kinematics and a base station, the positioning data from the GNSS receiver was found to be accurate up to a few centimetres, for speeds up to 3 m/s (faster was not tested). The demonstration device and the ROS software were also successfully tested by Fraunhofer FKIE, who mounted the device on a land robot.

The basic performance of the radiation detector module corresponds with performance claimed by the manufacturer. The detector responds quickly to changing radiation fields. Data produced was fully compliant with the data format standard IEC 63047, and can be shared with subscribers over the ROS network using the device driver developed by Fraunhofer FKIE. It is fair to believe that the demonstration device is rugged enough and suitable for field conditions, providing adequate environmental protection.

This report is Deliverable 4.3 of the ERNCIP RN Thematic Group for the 2018-2019 Work Programme.

# 1 Introduction

On 11 October 2018, the International Electrotechnical Commission (IEC) published a new international standard, IEC 63047<sup>[1]</sup>, specifying a data format for list-mode digital data acquisition used in radiation detection and measurement. IEC 63047 was developed under the lead of the JRC in the frame of Commission mandate M/487 (DG GROW). The pre-normative research for this standard was performed by the ERNCIP Thematic Group on Radiological and Nuclear threats to critical infrastructure. Input from Member State organisations qualified in radiation metrology was received via a Horizon2020 project. Equipment manufacturers were involved from the early stage, via an invitation published in the Official Journal of the European Union.

IEC 63047 is a binary standard which is applicable to data files and streams. The standard is specified using Abstract Syntax Notation One (ASN.1)<sup>[2]</sup>. The format supports various types of timestamped data and can be used in a wide range of applications involving radiation detection and measurement. It may also be used to represent data from other sensors than radiation detectors and supports positioning data from Global Navigation Satellite Systems (GNSS). The standard has a wide potential for CBRNE detection equipment, including robotics.

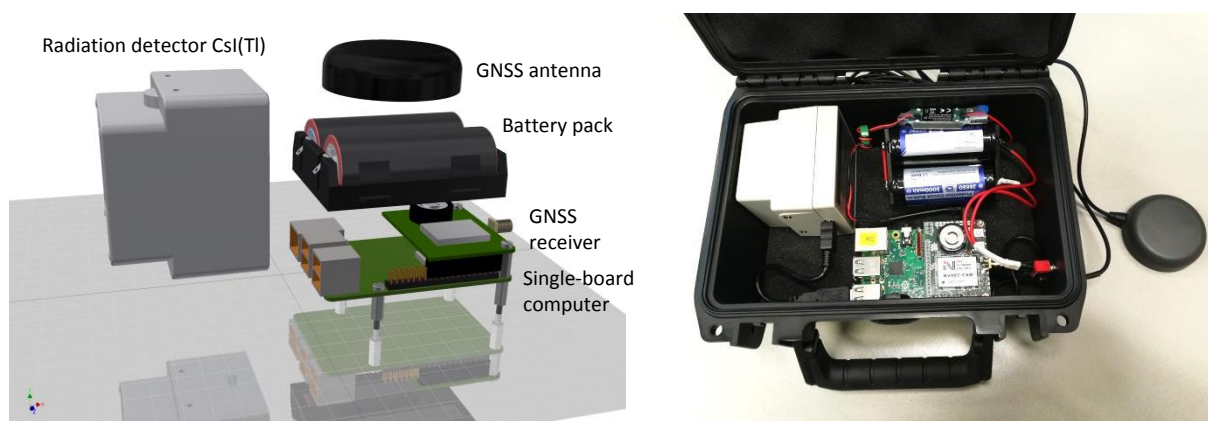
To facilitate the use of the standard, the JRC proposed and tested an open-source solution for encoding and decoding IEC 63047 messages. In addition, a demonstration device was developed from off-the-shelf components. The ERNCIP RN Robotics subgroup developed a software interface between IEC 63047 and the Robot Operating System (ROS). This report describes the demonstration device and discusses its performance with respect to fulfilling the requirements of the standard and its applicability to field conditions for robotics.

## 2 IEC 63047 demonstration device

### 2.1 Components

The IEC 63047 demonstration system was developed with components readily available on the market (Table 1). The device can be built for less than 3700 €, making it ideal to be used in training and education, but also for developing sensor networks which could for example be deployed in case of CBRNE incidents. The relatively low cost and weight makes it also suitable for robotics applications.

**Figure 1.** Components of the IEC 63047 demonstration device.



The device (Figure 1) consists of a single-board computer extended with a GNSS receiver board and an antenna. A radiation detection module is connected to the single-board computer via USB. Power is delivered from a battery pack via a switching regulator. Alternatively, a power bank may be used. Table 1 lists the components and indicative cost of the demonstration device. Similar systems may be constructed from alternative products.

**Table 1.** Components and indicative cost<sup>1</sup> of the IEC 63047 demonstration device.

Component	Example of a commercial product	Cost, excl. VAT
single-board computer	Raspberry® Pi 3B+ <a href="https://www.raspberrypi.org/">https://www.raspberrypi.org/</a>	€34
GNSS receiver	Aldebaran® from Dr Franz Fasching <a href="https://drfasching.com/">https://drfasching.com/</a>	€149
antenna	Tallysman® TW2410 <a href="http://www.tallysman.com/">http://www.tallysman.com/</a>	€104
radiation detector	Hamamatsu® C12137 or C12137-01 radiation detection module <a href="https://www.hamamatsu.com">https://www.hamamatsu.com</a>	€3270 or €4070
battery pack	2x type 26650 batteries and holder	€31
switching regulator	Reely® UBEC 5.5 – 26 V, 3 A	€11
case	SKB iSeries 0705-3B-C	€45
cables, hardware		€25
Total cost (excl. VAT)		€3669 or €4469

<sup>1</sup> Cost is provided for informative purpose only.

## 2.2 Operation

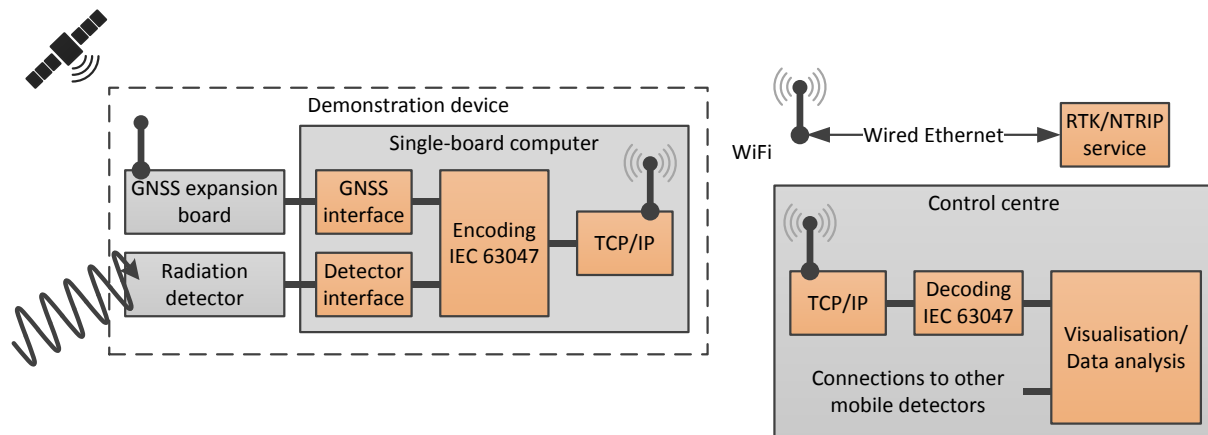
Figure 2 presents the functional layout of the demonstration environment. One or more mobile demonstration devices operate in a wireless network and send data to a control centre.

The radiation detector used in the demonstration device is capable of sending the energies of the observed photons to the single-board computer at a rate of ten times per second. The clock of the single-board computer is synchronised with Universal Coordinated Time via the GNSS connection. The data acquisition software combines the radiation data with the position and encodes the data into the IEC 63047 format, using the open-source software `asn1c` developed by Lev Walkin<sup>[3]</sup>.

Encoded data can be stored locally on the single-board or transmitted to the control centre over a wireless ROS connection. Alternatively, systems that do not use ROS can receive IEC 63047 data packages over a TCP socket. Note that, in this demonstration environment, a Wi-Fi network was used but in real scenarios the use of 3G/4G mobile communication (LTE) network is more appropriate. This is however merely a small technological difference.

The radiation detectors consist of a CsI(Tl) scintillator coupled to a multi-pixel avalanche photodiode. These photodiodes are operated in Geiger mode which results in a high internal gain that enables single photon detection. These devices also offer high photon detection efficiency, excellent timing resolution, low bias voltage operation, ruggedness, resistance to excess light, and immunity to magnetic fields<sup>[4]</sup>.

**Figure 2.** Layout of the demonstration environment.



To allow centimetre-accurate positioning, the GNSS expansion board needs an NTRIP connection to a RTK (Real-Time Kinematics) service. NTRIP is a protocol for standardised transmission of GNSS data over the internet. Real-time kinematic (RTK) was implemented with `rtkexplorer`<sup>[5]</sup>, which is a modified version of `RTKLib`<sup>[6]</sup> and allows the acquisition of centimetre-accurate satellite positioning information. At the JRC-Geel site, where the demonstration device was tested, the RTK service is provided by the Flemish Government (FLEPOS). Once the position of a local base station is accurately established, the NTRIP connection can be replaced by the local base station.



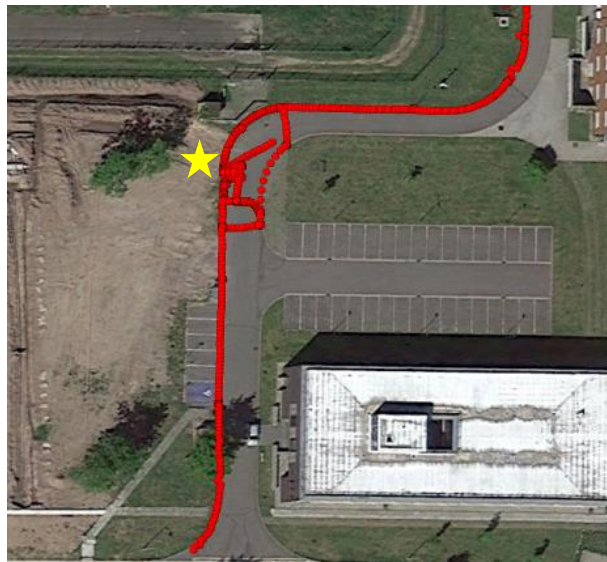
## 2.3 Test results

The demonstration device was tested at the JRC-Geel site. Special emphasis was put on testing the performance of the system from the point of view of fulfilling the requirements of the standard IEC 63047 and its applicability to field conditions for robotics. The accuracy of the satellite positioning and the performance in laboratory and field conditions was tested.

### 2.3.1 Positioning accuracy

In a first stage, the centimetre-accurate GNSS positioning was tested, without encoding data into the IEC 63047 format. A local outdoor Wi-Fi network was set up using a smartphone as mobile hotspot. The reference position of a 'base station' was first determined using the FLEPOS service. Using this base station instead of a virtual station determined by the FLEPOS service resulted in a very stable and accurate positioning signal.

**Figure 3.** Demonstrating centimetre-accurate positioning using real-time kinematic. (Satellite image from Google.)



The results of the positioning tests are shown in Figure 3. The smartphone that provides the Wi-Fi hotspot was located at the position of the yellow star. The demonstration device was moved around by a person following the border of the road, in order to compare the position with satellite images. The position of the demonstration device was logged and plotted using Google Earth<sup>[9]</sup>. The RTKLib software assigns a quality flag to the calculated position. The figure only shows the points that are flagged as 'Fixed'. These points are accurate up to a few centimetres. At the extremities of the track, the Wi-Fi signal was lost causing less accurate positioning data. High positioning accuracy could be sustained in open space at least 15 m away from buildings and trees and when moving at a maximum speed of 3 m/s. Faster speeds were not tested since not deemed necessary for Unmanned Ground Vehicles (UGVs). Experience from tests performed by University of Oulu shows that also for Unmanned Aerial Vehicles (UAVs), which may move faster, positioning accuracy up to a few centimetres can be achieved using the same technique: RTK referring to the known position of a base station.

### 2.3.2 Performance of the radiation detector in laboratory conditions

In a second stage, the basic performance of the radiation detector was tested in laboratory conditions, obviously without using GNSS positioning. Detector data was encoded in the IEC 63047 format and stored as a file on the memory card of the single-board computer. The files were then decoded and analysed. Table 2 summarises the properties of the radiation detector modules tested, including the lot numbers and serial numbers of the detectors actually tested. It was not the aim of these tests to fully characterise the response of the detectors, only the basic parameters were assessed.

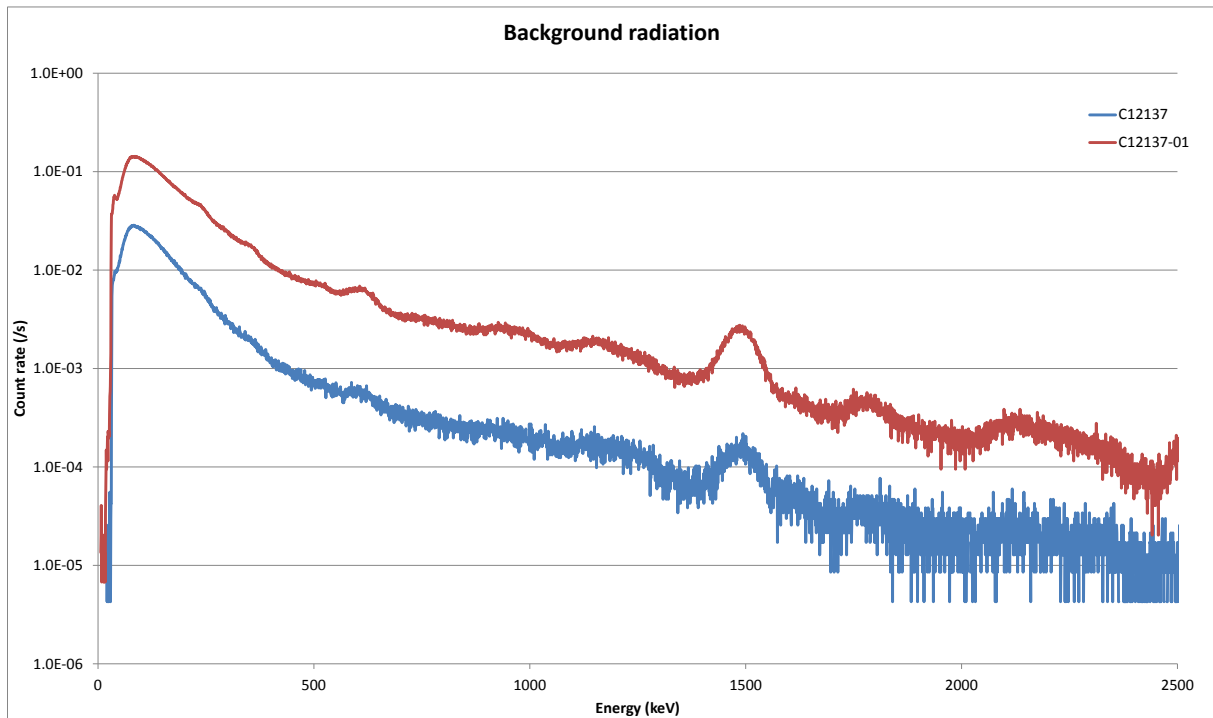
**Table 2.** Properties of the radiation detection module (from Hamamatsu C12137 series technical data sheet).

Parameter	Hamamatsu C12137	Hamamatsu C12137-01
Scintillator	CsI(Tl)	
Scintillator size	13 mm x 13 mm x 20 mm = 3 380 mm <sup>3</sup>	38 mm x 38 mm x 25 mm = 36 100 mm <sup>3</sup>
Mass	120 g	320 g
Counting efficiency <sup>2</sup> (for <sup>137</sup> Cs, 662 keV)	>40 cpm at 0.01 µSv/h (or >66 cps at 1 µSv/h)	>400 cpm at 0.01 µSv/h (or >666 cps at 1 µSv/h)
Energy resolution at 662 keV	< 8%	< 8.5%
Measurement range (dose rate)	0.01 µSv/h to 100 µSv/h	0.001 µSv/h to 10 µSv/h
Measurement error (dose rate)	< ±20%	
Lot number and serial number tested	Lot 14L S/N 0015	Lot 17E S/N 0008

Background spectra (Figure 4) were acquired over a period of 65 h for type C12137 and over 41 h for the bigger detector C12137-01. The logarithmic plot shows the expected <sup>40</sup>K peak at 1460 keV and the smaller peaks from the radionuclides in the <sup>238</sup>U decay series. The figure is expressed in units of count rate and confirms that the size of the scintillators differs by a factor of ten.

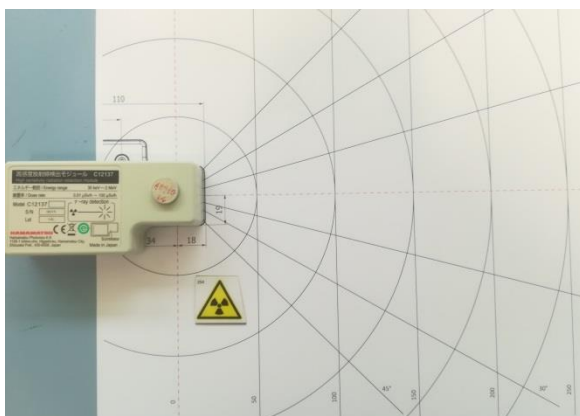
<sup>2</sup> cpm = counts per minute; cps = counts per second

**Figure 4.** Background spectra.

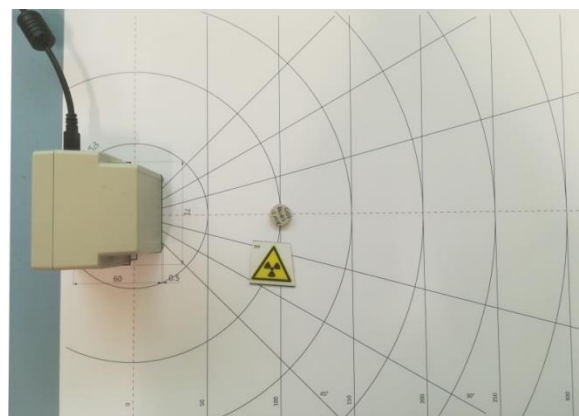


Measurements with a  $^{137}\text{Cs}$  source (Figure 5) were performed in order to verify the specifications provided by the manufacturer with respect to dose rate, counting efficiency and energy resolution. Also the response time of the detector was tested. Note that the geometry is not completely symmetric along the horizontal axis through the middle of the scintillator, which may lead to errors for close source-detector distances. The  $^{137}\text{Cs}$  source had an activity of about 91 kBq at the day of testing and was placed on top of the detector ('in contact') and at distances of 50 mm, 100 mm, 150 mm and 200 mm from the centre of the scintillator. Figure 6 shows the spectra recorded with the small detector (type C12137).

**Figure 5.** Basic performance tests of the radiation detectors in laboratory conditions.

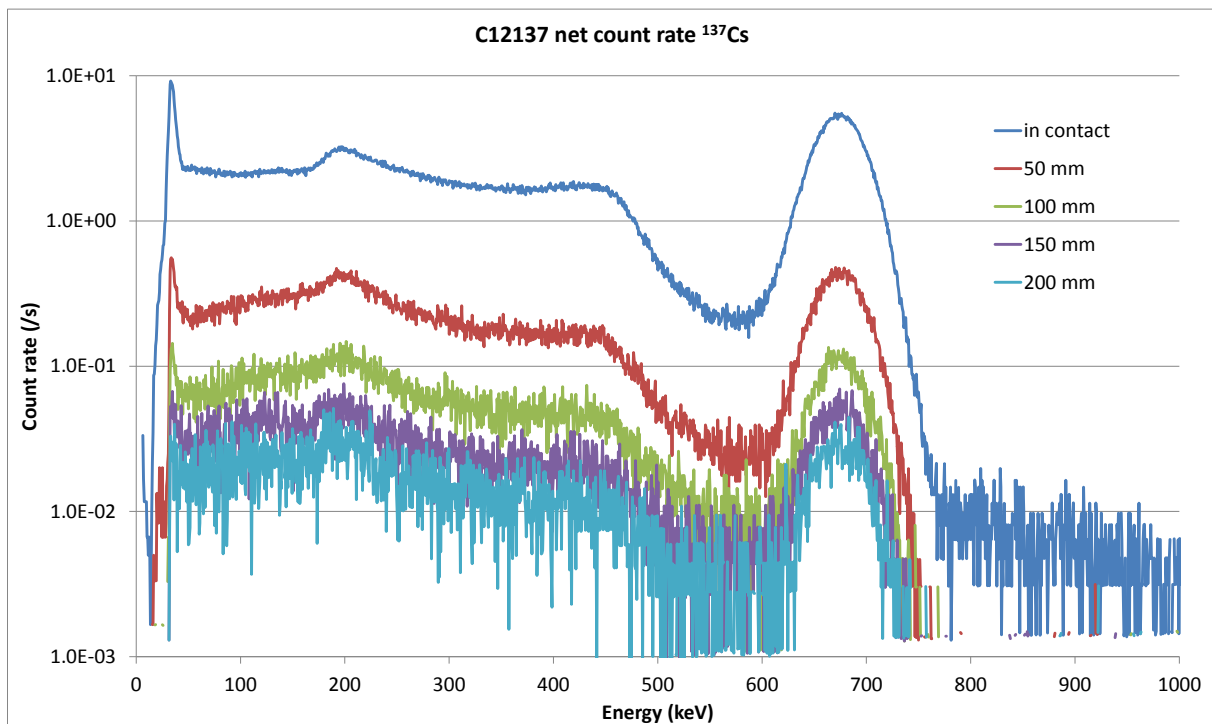


Hamamatsu type C12137-01



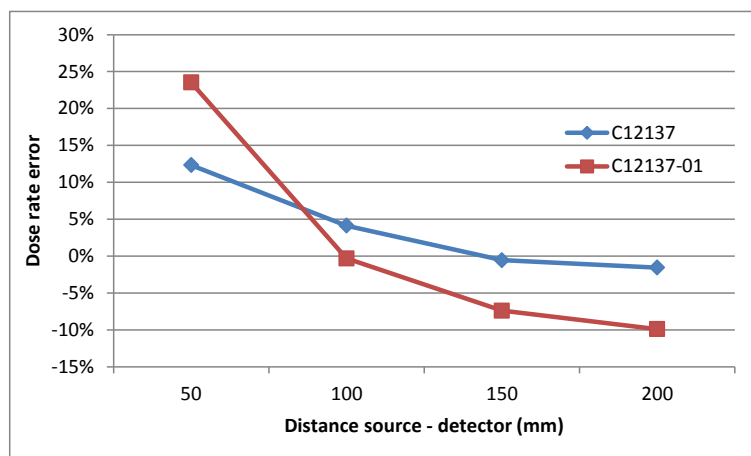
Hamamatsu type C12137

**Figure 6.** Net (background corrected) energy spectra recorded with a  $^{137}\text{Cs}$  source at different distances to the detector.



The correctness of the dose rate (from 662 keV gamma radiation emitted by  $^{137}\text{Cs}$ ) was verified by comparing the measured dose rate with a theoretical dose rate calculated using the Nucleonica 'Dosimetry and Shielding++' application<sup>[10]</sup>. Figure 7 shows that the dose rate is correct within the claimed  $\pm 20\%$ , except for the larger detector with the source at 50 mm distance, which yielded an error of 24%.

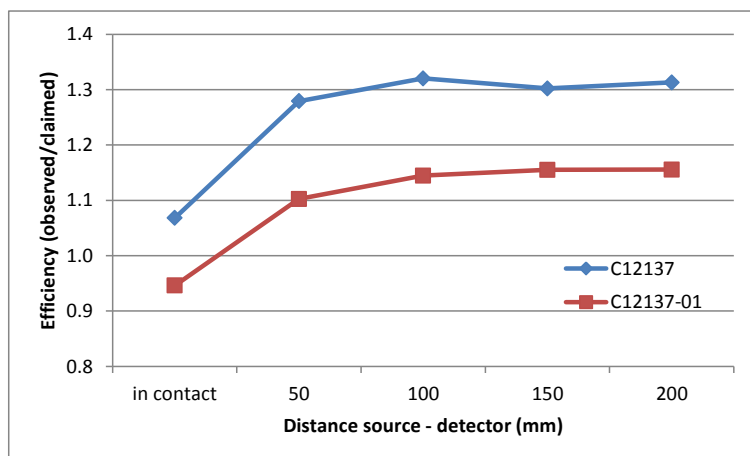
**Figure 7.** Error on the dose rate.



The counting efficiency was determined by subtracting (in counts per second) the background spectrum from the energy spectrum obtained with the  $^{137}\text{Cs}$  source, and then integrating the net spectrum for energies larger than 43 keV. The resulting count rate (attributed to  $^{137}\text{Cs}$  only) is then divided by the measured dose rate, yielding a figure of efficiency (counts per second per 1  $\mu\text{Sv/h}$ ). Figure 8 plots the ratio of this figure to the claimed (minimum) efficiency. The test was performed at different distances from the source to the detector. The figure shows that the efficiency is at least as good as

claimed, except for the larger detector with the source in contact. In fact, for this particular measurement the net dose rate exceeded the maximum dose rate of 10  $\mu\text{Sv/h}$  for C12137-01. It is therefore justified to ignore this point and confirm the performance with respect to counting efficiency.

**Figure 8.** Ratio of the observed counting efficiency versus the claimed efficiency.



At count rates above 1500 per second, both detectors suffer from pile-up. This effect can be observed from the net (background corrected) spectra recorded with the  $^{137}\text{Cs}$  source close to the detector. In principle, apart from statistical fluctuations in the background radiation, there should not be any counts in the spectra at energies beyond the full-energy Gaussian peak. Figure 9 was recorded with the small detector and shows an elevated number of counts at energies higher than about 750 keV when the source is in contact with the detector. As can be expected, the effect is larger for the larger detector, as demonstrated by Figure 10 where pile-up is still slightly present at a distance of 50 mm.

**Figure 9.** Net count rate spectrum showing pile-up of events when the source is in contact with the small detector.

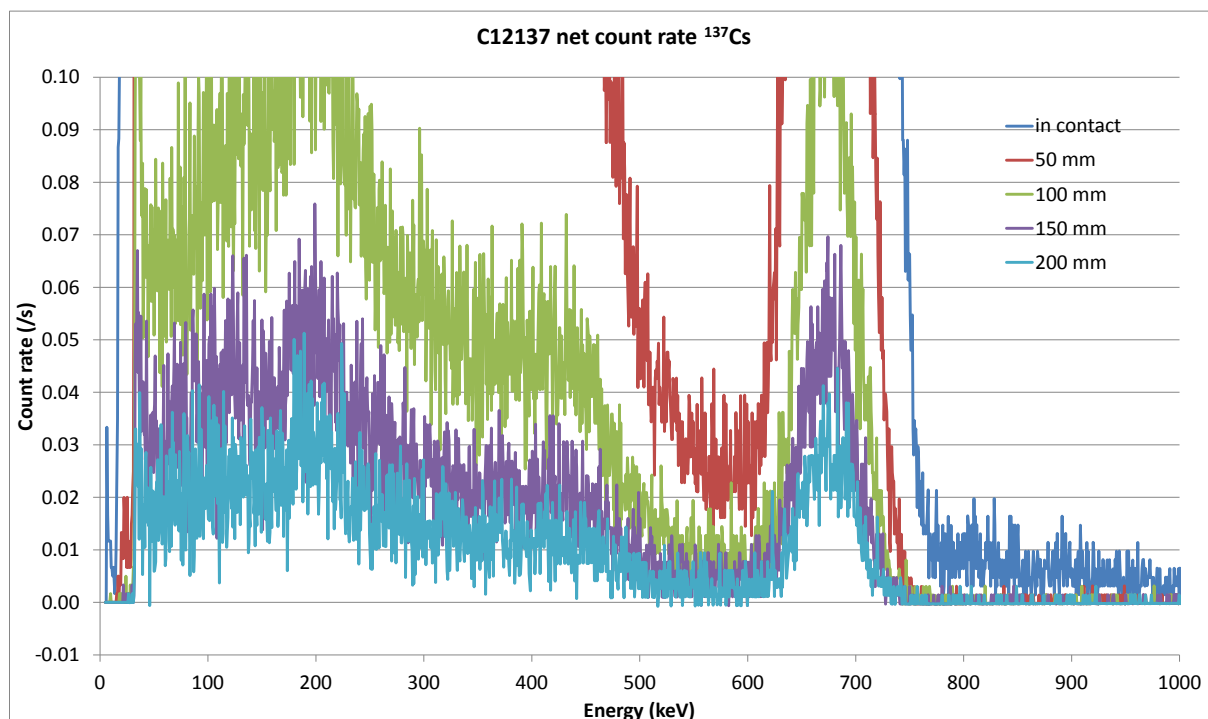
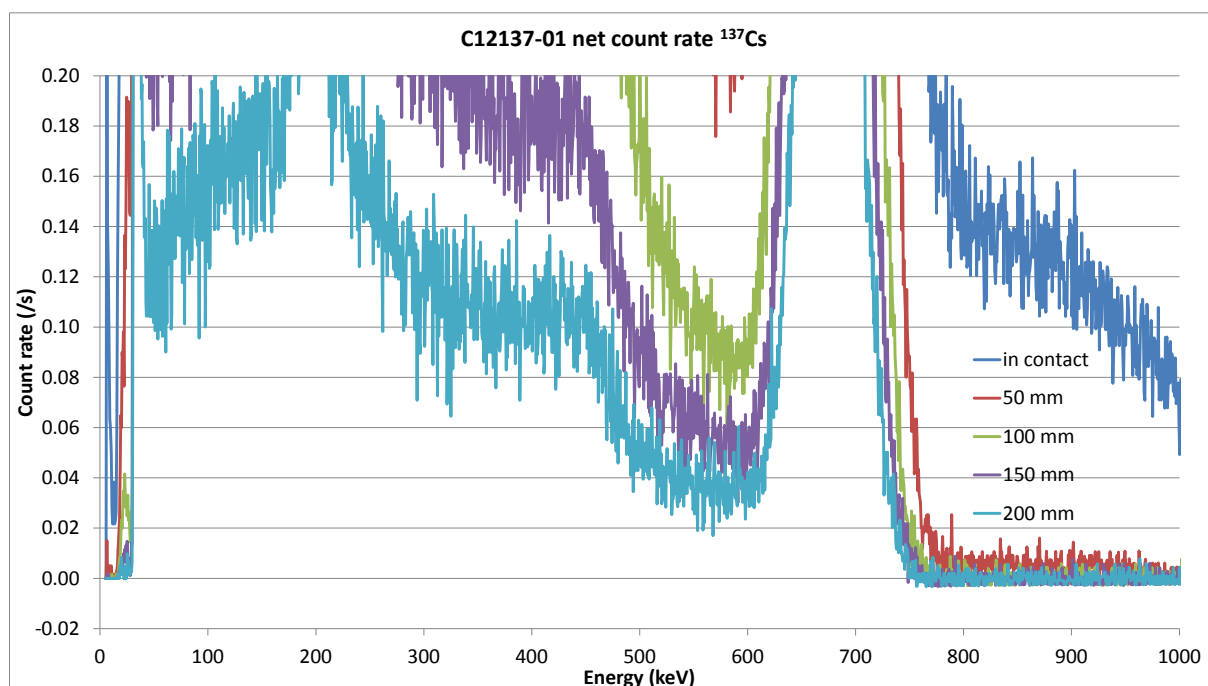


**Figure 10.** Net count rate spectrum showing pile-up of events when the source is in contact with the larger detector. The pile-up effect is also present when the source is at a distance of 50 mm.

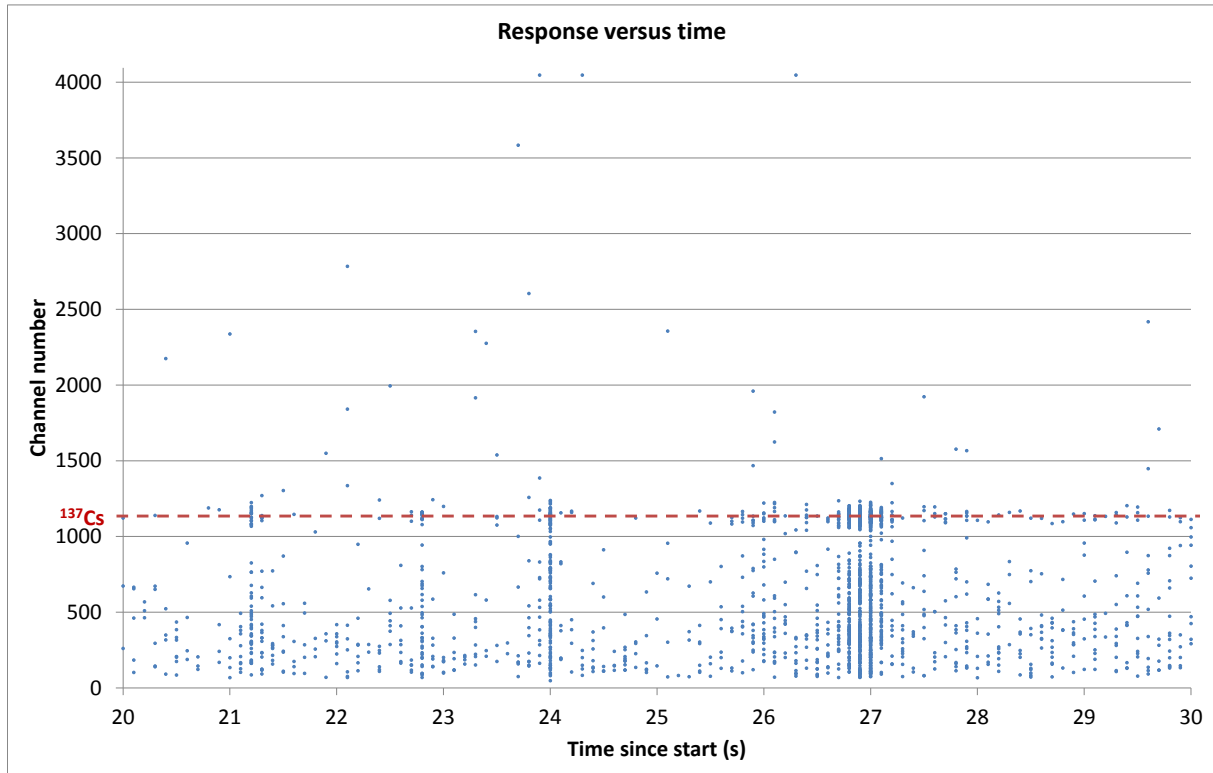


The pile-up effect is caused by the detector electronics not being fast enough to remove all charges associated to the light observed from one gamma-ray interaction before the next gamma-ray interacts.

Earlier experience with robot-ported dose rate meters shows a delay in the response of the detector when exposed to a quickly changing radiation field, for example as observed when the robot moves quickly over a point source. The effect is caused due to the integration time of the detector. Smaller and lighter detectors are less sensitive to

radiation and therefore a time averaging is needed to yield a reasonably stable dose rate reading. The detector used in the demonstration device is a spectrometric device that sends data at a rate of ten times per second. To test the response time, the detector was placed at a fixed location in the lab and a  $^{137}\text{Cs}$  source was manually moved over the detector at a high speed. The timestamp and channel number of each gamma-ray interaction observed in the detector are stored and plotted on Figure 11. The position of the  $^{137}\text{Cs}$  full-energy peak is indicated by the red dashed line.

**Figure 11.** Response versus time to a quickly moving  $^{137}\text{Cs}$  source.



The figure shows that indeed 10 times per second data is acquired. At 21.2 s, 22.8 s and 24 s after the start of the measurement the source was passing a few cm above the detector. Many events are recorded within the small time interval of 0.1 s. Around 27 s, the source was moved slower, resulting in even more events, spread over a total time interval of about 0.5 s. From this experiment we conclude that the detector in the demonstration device does not show a delay in the response.

Finally, the energy resolution measured at 662 keV was slightly better than the claimed values.

### 2.3.3 Field tests

In a third and final stage, the complete demonstration device (including the radiation detector and GNSS receiver) was tested in outdoor conditions. Figure 12 shows the device with the GNSS antenna placed on a tripod. Both detector and positioning data were encoded into the IEC 63047 data format and stored on the memory card of the single-board computer, at a rate of 10 times per second. Compliance of the generated data files with the data format standard was confirmed by importing the file into the software ASN1 Studio<sup>[7]</sup>. Annex 1 contains an extract of the data file, converted to a human-readable format.

**Figure 12.** Demonstration device in field test.



Similar as in the first test, accurate positioning was achieved. The limited test shows that the demonstration device appears to be fit for purpose. Additional tests could include performance tests according to established standards, such as environmental, stability or sensitivity. Elaborate testing however is out of the scope of this work.



### 3 Integration in ROS

#### 3.1 ROS framework

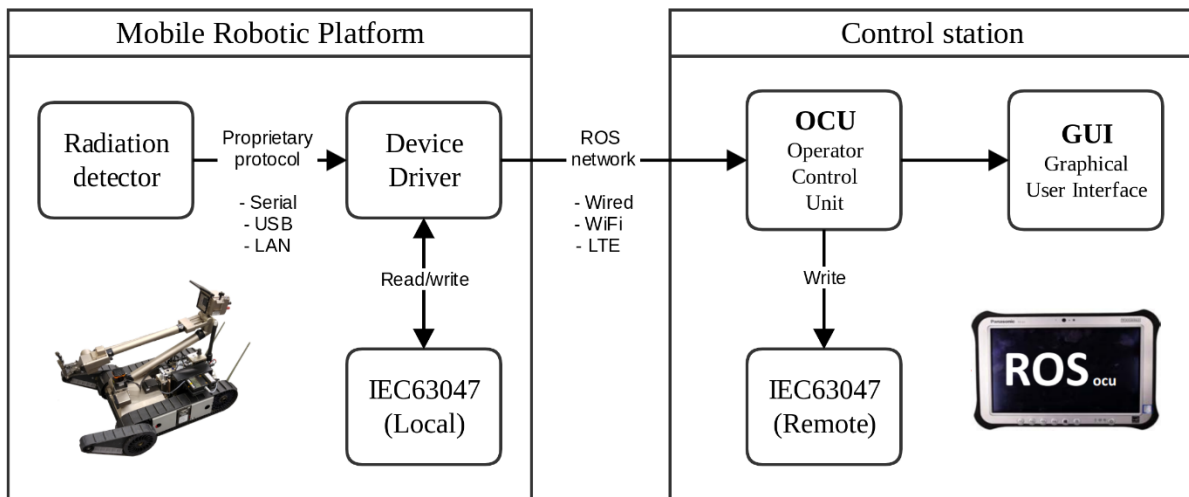
Robotic systems are generally composed by heterogeneous mobile robots and Operator Control Units (OCU) connected by wireless interfaces such as Wi-Fi or LTE. The communication between all involved parts is handled by ROS, enabling bi-directional data transfer using serialized messages through TCP/UDP socket connections.

Establishing a wireless communication network is not straightforward. Usually, wireless data communication is not very reliable, has limited band-width and therefore is often restricted to ROS messages. The robotic platform should locally process the acquired data and only use the ROS network to transmit data which is required for the mission.

In the ROS framework, all processes that perform computation are called nodes and the software is organised using packages that contain source code, nodes and configuration files. ROS nodes communicate to each other by interchanging 'typed-fields messages', defined by a simplified message description language that enables automatic code generation. The fields of the messages are created using standard built-in types such as boolean, 8-bit integer or 64-bit floating point numbers.

For integrating the demonstration device in robotic applications, Fraunhofer FKIE created a software interface using ROS packages based on the encoding/decoding solution provided by the JRC. The developed software interface is divided into two main components: A multifunctional device driver node that is executed inside the mobile robotic platform and an OCU driver node, running in a control station by the end operator/user (Figure 13). Both nodes are discussed in the following sections, after which performance tests are discussed.

**Figure 13.** Layout of the ROS integration.



### 3.2 ROS device driver node

The radiation detector measures periodically (up to ten times per second) dose and gamma rate, as well as the energy spectrum. The measurements are requested by the device driver using a vendor-specific protocol and interface. In case of the Hamamatsu detector of the demonstration device, communication is performed over an USB connection. Simultaneously, the device driver receives geolocation data from the attached GNSS device using an emulated serial interface, containing information about current latitude, longitude, altitude and time.

The device driver node runs on the mobile robotic platform. The driver serializes the measurements and geolocation data into a measurement-generic ROS message named [MeasurementLocated], and publishes it on the ROS network. The definition of the generic message is shown in Table 3. It is worth noting that multiple nodes, for instance OCUs or even other robots, may subscribe simultaneously to receive the published data.

**Table 3.** ROS Message definition for collected measurements.

Message Name	Fields		Description
	Type	Name	
MeasurementLocated	Measurement	measurement	Geo-location
	float64	latitude	
	float64	longitude	
	float64	altitude	
Measurement	Header	header	Measurement time stamp
	string	device_name	Custom name of the device
	string	device_designation	Device manufacturing name
	string	classification	Classification of the device (if applicable)
	Value[]	values	Measurement values
Value	string	sensor	Name of the sensor
	string	source	Source of the sensor data, e.g. wind, rain or other
	string	type	Type of sensor data, e.g. speed, duration, intensity
	float64[]	value	Single measurement or a spectrum of values
	string	unit	Measurement units
	float64	min	Minimum value (if available)
	float64	avg	Average value (if available)
	float64	max	Maximum value (if available)
	string	info	Additional information

The device driver also allows encoding the measurements and geolocation data into the IEC 63047 format. The binary IEC 63047 messages can then be stored in a local file or published on the ROS network using a built-in message of type [std\_msgs/ByteMultiArray], which serves as a binary container. Local storage on the robot is particularly useful when the network connection gets interrupted and/or the communication with an OCU is not available. Considering the design criteria in ROS, it is strongly advisable to avoid generic message types, because they do not convey any semantic meaning about their content. In principle, this design rule is violated when IEC 63047 encoded data is transmitted over the ROS network using the binary container. Therefore, the use of the built-in message of type [std\_msgs/ByteMultiArray] is only

acceptable when the subscribers have the prior knowledge that the data is encoded into the IEC 63047 format.

The driver node supports both approaches simultaneously (typed-fields messages and the binary-container). Selecting among them is application dependent. For instance, if the application only requires plotting the measured data in the control station, the message type [MeasurementLocated] is more appropriate because it does not require any additional processing. However, if the application involves integration with additional systems, such as databases or external devices supporting the IEC 63047 format, the binary-container message is more convenient. A comparison between the performances of both is made in 3.4.

### 3.3 ROS OCU driver node

The OCU driver node runs on the control station. ROS messages are streamed to the OCU subscriber node(s), which extracts the corresponding measurements and geolocation data. Next, it is possible to visualize the data using a graphical user interface (GUI) or (if required) to encode the data into the IEC 63047 format and store in a local files or stream over a connection socket. Encoding to IEC 63047 is useful for integration with external systems or databases.

### 3.4 Performance test

Although both approaches (typed-fields messages and the binary-container) are technically feasible, some additional performance and design considerations need to be taken before selecting any of them.

The IEC 63047 standard requires the use of the C-OER encoding rule (Canonical Octet Encoding Rule<sup>[8]</sup>). Other data formats, for example the IEC 62755 format, uses XML encoding, which is human readable. Because IEC 63047 is specified using ASN.1 (which decouples the specification of the data format from the encoding rule), it is easy to read C-OER encoded data and convert the data using another encoding rule. For comparison, tests were performed using XER (XML Encoding Rule) and BER (Basic Encoding Rule), in addition to C-OER. The encoding rule determines the size of the encoded data and therefore the required bandwidth for transmitting a measurement. It is important to realise that the requirements on resources (memory and computing time) are also affected by the encoding rule. During the development of IEC 63047 it was found that from all the ASN.1 encoding rules, C-OER offered the best compromise between encoding size, speed and memory use.

A performance test was executed to compare the required bandwidth between the four message definitions. Measurements of the background radiation were collected by the radiation detector (Hamamatsu type C12137-01). The ROS device driver node runs on the demonstration device and publishes the data while the ROS OCU driver node on the control station subscribes to read the data. The bandwidth usage during the test is presented in Table 4.

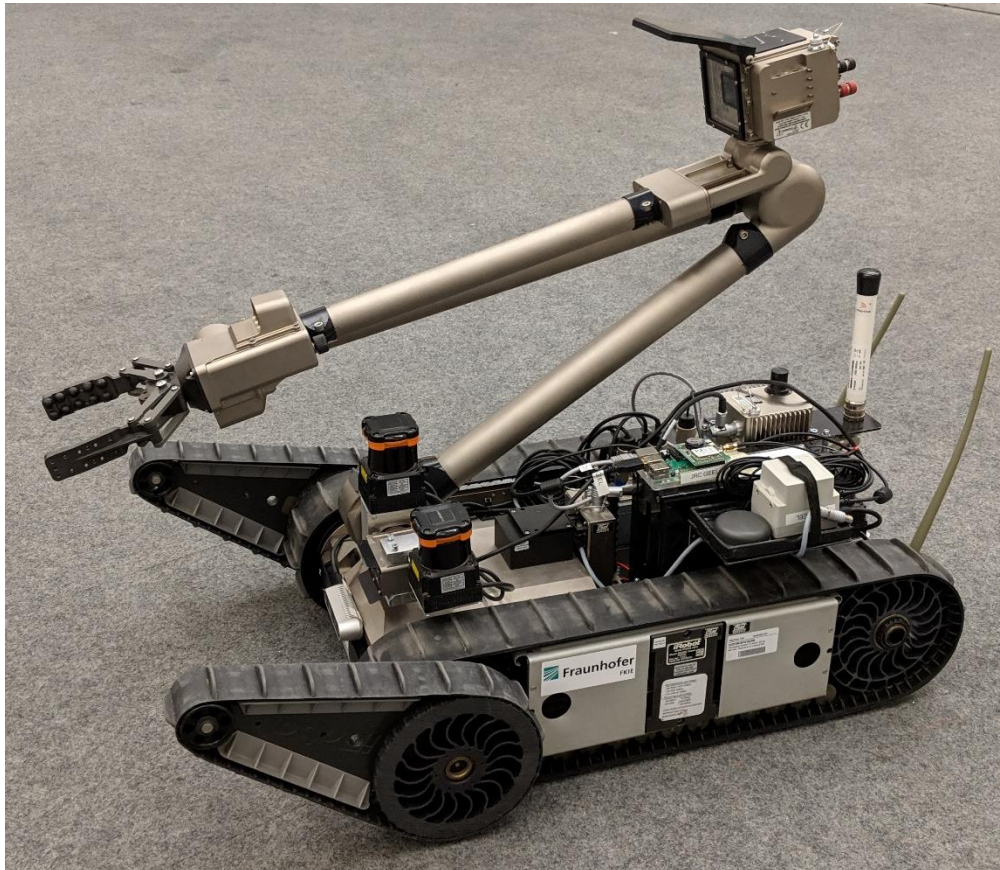
**Table 4.** Bandwidth usage during the performance test.

ROS Message Type	Encoding rule	Average Bandwidth Used (1 kB = 1024 B)
typed-fields message [MeasurementLocated]	ROS serialization	32 kB/s
binary container [std_msgs/ByteMultiArray] with IEC 63047 data	C-OER	9 kB/s
	BER	13 kB/s
	XER	235 kB/s

The human-readable XER encoding requires about seven times more bandwidth than the [MeasurementLocated] type while C-OER encoding of IEC 63047 data requires about three times less bandwidth.

Finally, the developed ROS integration packages were successfully tested using the demonstration device mounted on an iRobot Packbot, showed in Figure 14. The developed package can also be executed directly on the robot computer, without using explicitly the demonstrator device. In this configuration, the radiation detector is connected to the robot computer using USB and the geolocation data is provided by the integrated robot GPS.

**Figure 14.** Demonstration device mounted on a mobile robotic platform.



The device driver developed by Fraunhofer FKIE already supports IEC 63047 files as input, enabling future integration of radiation detectors that also supports this standard. This is particularly important for improving and simplifying the integration of new radiation detection systems.

## Conclusions

The JRC developed a device from off-the-shelf components to demonstrate the use of the data format standard IEC 63047. The demonstration device implements a solution for encoding data into the standard format using existing open-source code. The demonstration device consists of a single-board computer, a spectrometric radiation detector and a GNSS receiver which enables real-time-kinematics to achieve centimetre accurate positioning.

The radiation detector is capable of acquiring detector data up to a maximum rate of 10 times per second. The detector data is combined with the positioning information and encoded into the IEC 63047 format. The JRC developed code for the interface with the radiation detector. The JRC code stores the encoded data on the memory card of the single-board computer. Detector data may consist of gamma count rate, spectrum or dose rate. Fraunhofer FKIE extended the detector interface to a ROS device driver, capable of sending the data to the operator control unit over the ROS network. The device driver can be extended with interfaces to other radiation detectors than the one used in the demonstration device.

Tests performed at the JRC-Geel site assessed the performance of the demonstration device in laboratory and field conditions. Radiation background measurements and measurements with a  $^{137}\text{Cs}$  were performed in laboratory conditions. Using real-time kinematics and a base station, the positioning data from the GNSS receiver was found to be accurate up to a few centimetres, for speeds up to 3 m/s (faster was not tested). Compliance of the generated data against IEC 63047 was verified.

The demonstration device and the ROS software were also successfully tested by Fraunhofer FKIE, who mounted the device on a UGV.

In general, the demonstration device performs as expected. The basic performance of the radiation detector module corresponds with performance claimed by the manufacturer. The demonstration device responds quickly to changing radiation exposure. Data produced was fully compliant with the data format standard IEC 63047, and can be shared with subscribers over the ROS network using the device driver developed by Fraunhofer FKIE. Profound tests against established standards were not performed due to the limited resources available. Nevertheless, it is fair to believe that the device is rugged enough and suitable for field conditions, providing adequate environmental protection.

Further tests where several demonstration devices operate together are planned by the JRC in the exploratory research activity 2018-ER-A32 'list-mode robotics trial'. Robots will move the demonstration device around a test site where a radioactive source is hidden. The aim of the research project is to assess the added value of acquiring data in list-mode in search operations.

## References

- [1] IEC 63047, Edition 1.0, 2018-10, *Nuclear instrumentation – Data format for list mode digital data acquisition used in radiation detection and measurement*
- [2] ISO/IEC 8824-1:2015, ITU-T X.680, *Information technology – Abstract Syntax Notation One (ASN.1): Specification of basic notation*
- [3] Walking, L., *asn1c*, available from GitHub, <https://github.com/vlm/asn1c>
- [4] Hamamatsu Multi Pixel Photon Counter, (<https://www.hamamatsu.com/eu/en/product/optical-sensors/mppc/index.html>)
- [5] *rtkexplorer*, Exploring high precision GPS/GNSS with low-cost hardware and software solutions, <http://rtkexplorer.com/>
- [6] *RTKLib*: An Open Source Program Package for GNSS Positioning, <http://www.rtklib.com/>
- [7] *ASN1 Studio*®, OSS Nokalva, <https://www.oss.com>
- [8] ISO/IEC 8825-7:ITU-T X.696, *Information technology – ASN.1 encoding rules: Specification of Octet Encoding Rules (OER)*
- [9] Google Earth (<https://earth.google.com>)
- [10] Nucleonica Dosimetry and Shielding++ web application (<https://www.nucleonica.com/Application/ShieldingPlus.aspx>)

## List of abbreviations and definitions

ASN.1	Abstract Syntax Notation One
BER	Basic Encoding Rule
CBRNE	Chemical, Biological, Radioactive, Nuclear and Explosive
C-OER	Canonical Octet Encoding Rule
cpm	counts per minute
cps	counts per second
CsI(Tl)	Caesium-iodide, doped with thallium (a scintillator material sensitive to gamma radiation)
ERNICIP	European Reference Network for Critical Infrastructure Protection <a href="https://erncip-project.jrc.ec.europa.eu/">https://erncip-project.jrc.ec.europa.eu/</a>
FLEPOS	The Flemish positioning service provides a network of permanent GNSS stations, including services for RTK GNSS.
GNSS	Global Navigation Satellite System (GPS, GLONASS, Galileo and BeiDou-2)
GPS	Global Positioning System
GUI	Graphical User Interface
IEC	International Electrotechnical Commission
LTE	Long Term Evolution, a high performance data transfer system used in 4G
NTRIP	Networked Transport of RTCM 3.x data via Internet Protocol: standardised transmission of GNSS data over the internet
OCU	Operator Control Unit
ROS	Robot Operating System
RTCM	Radio Technical Commission for Maritime Services is an international standards organization
RTK	Real-Time Kinematics
TCP	Transmission Control Protocol
UAV	Unmanned Aerial Vehicle
UDP	User Datagram Protocol
UGV	Unmanned Ground Vehicle
USB	Universal Serial Bus
XER	XML Encoding Rule
XML	Extensible Markup Language

## List of figures

<b>Figure 1.</b> Components of the IEC 63047 demonstration device. ....	5
<b>Figure 2.</b> Layout of the demonstration environment. ....	6
<b>Figure 3.</b> Demonstrating centimetre-accurate positioning using real-time kinematic. (Satellite image from Google.) ....	7
<b>Figure 4.</b> Background spectra. ....	9
<b>Figure 5.</b> Basic performance tests of the radiation detectors in laboratory conditions. ...	9
<b>Figure 6.</b> Net (background corrected) energy spectra recorded with a $^{137}\text{Cs}$ source at different distances to the detector. ....	10
<b>Figure 7.</b> Error on the dose rate. ....	10
<b>Figure 8.</b> Ratio of the observed counting efficiency versus the claimed efficiency. ....	11
<b>Figure 9.</b> Net count rate spectrum showing pile-up of events when the source is in contact with the small detector. ....	12
<b>Figure 10.</b> Net count rate spectrum showing pile-up of events when the source is in contact with the larger detector. The pile-up effect is also present when the source is at a distance of 50 mm. ....	12
<b>Figure 11.</b> Response versus time to a quickly moving $^{137}\text{Cs}$ source. ....	13
<b>Figure 12.</b> Demonstration device in field test. ....	14
<b>Figure 13.</b> Layout of the ROS integration. ....	15
<b>Figure 14.</b> Demonstration device mounted on a mobile robotic platform. ....	18



## List of tables

<b>Table 1.</b> Components and indicative cost of the IEC 63047 demonstration device. ....	5
<b>Table 2.</b> Properties of the radiation detection module (from Hamamatsu C12137 series technical data sheet). ....	8
<b>Table 3.</b> ROS Message definition for collected measurements. ....	16
<b>Table 4.</b> Bandwidth usage during the performance test. ....	17

## Annexes

### Annex 1. IEC 63047 data acquired during field tests

The data presented in this annex was acquired and stored in the IEC 63047 format by the demonstration device. The binary file was opened with the software package ASN1 Studio<sup>[7]</sup> and then saved as a text file in the ASN.1 value notation syntax. The most relevant parts of the text file are included as an example. The comments (starting with --) have been added manually to explain the meaning of the data elements.

An IEC 63047 data file is a sequence of values of the `Listmodedata` data type, encoded using the C-OER encoding rule. The `Listmodedata` data type is a choice between the `Header` type, the `Eventlist` type and the `Footer` type. The first value in the file is always of the `Header` type, and is followed by values of the `Eventlist` type. Finally, the last value in the file is of the `Footer` type.

```
value1 Listmodedata ::= header : {
  standardID "IEC 63047 Ed. 1.0", -- Fixed element
  listModeDataID "17E0008", -- Identifies the data. (Here: lot and serial number.)
  listModeDataPart 0, -- This is the first part of the data
  listModeDataNParts 1, -- There is only one part
  measSetupID "Hamamatsu C12137", -- Identification of the measurement setup
  measSetupDescription "Hamamatsu C12137 over USB", -- Description of the measurement setup
  iec62755 single : NULL, -- There is no associated file in the IEC 62755 format
  radSource "Background radiation", -- The source of radiation is natural background
  start {
    date-time "2019-05-14T13:23:32Z", -- The start of the measurement, in UTC
    fractional-seconds 6.41E-1 -- Precise start was 0,641 seconds after
  },
  deviceList { -- The list of devices (here only one)
    {
      name "Radiation detector module",
      manuf "Hamamatsu",
      model "C12137",
      serial "17E0008" -- Here a combination of lot number and serial number
    }
  },
  channelList { -- The list of channels (here only one)
    {
      deviceID 0, -- Channel belongs to the first device
      kind physickind, -- This is a physical channel (real detector channel)
      physicalChannel 0, -- Number of the channel on the device
      name "CH0",
      description "Multi-pixel photon counter coupled to a CsI(Tl) scintillator",
      parameters "[comparator threshold][30][keV];[lower limit energy range][30][keV];
        [higher limit energy range][ 2.000][MeV];[conversion factor][ 1.000][uSv/h];
        [ADC to keV][1000][keV];[energy threshold][60][keV]", -- Set of configuration parameters
      delay 0, -- No time delay applied
      adcSamplingRate int : 0, -- Not applicable here
      adcBitResolution 12, -- There are 4096 (2^12) bins in the energy histogram
      clockFrequency int : 10, -- Timestamp clock runs at 10 Hz (one tick is 0,1 s)
      eventPropertyList { -- Event types to expect in the Eventlist, and their properties
        eventPulseProperty : {
          description "CH0 records TimeStamp and pulse height",
          valueDescriptionList {
            "Pulse height"
          }
        },
        eventGeoProperty : {
          description "RTKDEMO5 b31"
        }
      }
    }
  }
}
```

```

value2 Listmodedata ::= eventList : {
  listModeDataID "17E0008", -- Identifies the data (same as in Header)
  listModeDataPart 0, -- This is part 1 of the data
  id 0, -- This is the first Eventlist
  eventList {
    eventPulse : { -- A gamma ray in bin 1675 was detected 0,7 seconds after start
      channelID 0,
      timeStamp 7, -- To multiply with the inverse of clockFrequency from Header
      valueList {
        int : 1675
      }
    },
    -- Other events of the eventPulse type have been omitted
    eventPulse : { -- A gamma ray in bin 163 was detected 2,9 seconds after start
      channelID 0,
      timeStamp 29,
      valueList {
        int : 163
      }
    },
    eventGeo : { -- The position at 3,2 seconds
      channelID 0,
      timeStamp 32,
      position geographicPoint : {
        latitude 5.1196566162E+1,
        longitude 5.041901482E+0,
        datum "WGS-84"
      }
    },
  }
}

value3 Listmodedata ::= eventList : {
  listModeDataID "17E0008", -- Identifies the data (same as in Header)
  listModeDataPart 0, -- This is part 1 of the data
  id 1, -- This is the second Eventlist (starts counting from 0)
  -- Events are omitted here
}

-- Eventlists are omitted here

value1418 Listmodedata ::= eventList : {
  listModeDataID "17E0008", -- Identifies the data (same as in Header)
  listModeDataPart 0, -- This is part 1 of the data
  id 1416, -- This is the 1417th Eventlist (starts counting from 0)
  -- Events are omitted here
}

value1419 Listmodedata ::= footer : { -- This is the end of the data
  listModeDataID "17E0008", -- Identifies the data (same as in Header)
  listModeDataPart 0, -- This is part 1 of the data
  lastEventListid 1416 -- The id of the last event list was 1416
}

```



## **GETTING IN TOUCH WITH THE EU**

### **In person**

All over the European Union there are hundreds of Europe Direct information centres. You can find the address of the centre nearest you at: [https://europa.eu/european-union/contact\\_en](https://europa.eu/european-union/contact_en)

### **On the phone or by email**

Europe Direct is a service that answers your questions about the European Union. You can contact this service:

- by freephone: 00 800 6 7 8 9 10 11 (certain operators may charge for these calls),
- at the following standard number: +32 22999696, or
- by electronic mail via: [https://europa.eu/european-union/contact\\_en](https://europa.eu/european-union/contact_en)

## **FINDING INFORMATION ABOUT THE EU**

### **Online**

Information about the European Union in all the official languages of the EU is available on the Europa website at: [https://europa.eu/european-union/index\\_en](https://europa.eu/european-union/index_en)

### **EU publications**

You can download or order free and priced EU publications from EU Bookshop at: <https://publications.europa.eu/en/publications>. Multiple copies of free publications may be obtained by contacting Europe Direct or your local information centre (see [https://europa.eu/european-union/contact\\_en](https://europa.eu/european-union/contact_en)).

## The European Commission's science and knowledge service

Joint Research Centre

### JRC Mission

As the science and knowledge service of the European Commission, the Joint Research Centre's mission is to support EU policies with independent evidence throughout the whole policy cycle.



**EU Science Hub**

[ec.europa.eu/jrc](https://ec.europa.eu/jrc)



@EU\_ScienceHub



EU Science Hub - Joint Research Centre



Joint Research Centre



EU Science Hub



Publications Office

doi:10.2760/041774

ISBN 978-92-76-08684-0